

## $\beta$ -phase tungsten nanorod formation by oblique-angle sputter deposition

Tansel Karabacak,<sup>a)</sup> Anupama Mallikarjunan, Jitendra P. Singh, Dexian Ye, Gwo-Ching Wang, and Toh-Ming Lu

*Department of Physics, Applied Physics and Astronomy, Rensselaer Polytechnic Institute, Troy, New York 12180-3590*

(Received 19 May 2003; accepted 20 June 2003)

We report the creation of an unusual simple cubic  $\beta$ -phase W(100) nanorods with a pyramidal tip having four (110) facets using an oblique-angle sputter deposition technique with substrate rotation (also known as glancing-angle deposition). During the oblique-angle deposition, both  $\beta$ -phase W(100) and  $\alpha$ -phase W(110) islands exist at the initial stages of growth. The  $\beta$ -phase W(100) islands grow taller due to the lower adatom mobility on these islands. The taller islands survive in the competition and form isolated nanorods in the later stages of growth. This is in contrast to the sputter deposition at normal incidence, where only the thermodynamically stable bcc  $\alpha$ -phase W(110) polycrystalline films were formed when the film grows to a certain thickness. © 2003 American Institute of Physics. [DOI: 10.1063/1.1618944]

Tungsten films have been the subject of intense research due to their importance in a number of technological applications, for example, field emitters,<sup>1</sup> photonic crystals,<sup>2</sup> diffusion barriers in semiconductor interconnect structures,<sup>3,4</sup> absorbing layers in x-ray masks,<sup>5</sup> and x-ray mirrors.<sup>6</sup> Depending on the growth conditions and thickness of the films, normal incidence sputter deposition of tungsten films can give rise to either the  $\alpha$ -phase W, which has the equilibrium bcc structure, or the metastable  $\beta$ -phase W, which has an A15 (cubic) structure, or a mixture of both phases.<sup>7–11</sup> The lattice constants are 3.16 and 5.04 Å for  $\alpha$ -W and  $\beta$ -W, respectively. These two phases may have very different properties; for example, the measured resistivity of  $\beta$ -W film is an order of magnitude higher than that of the  $\alpha$ -W film.<sup>3</sup> It was suggested that oxygen incorporation might play a role in the formation of the metastable  $\beta$ -W. In the normal incidence sputter deposition of tungsten film, the lattice constant of the  $\beta$ -W phase monotonically decreases with increasing sputtering time until the  $\beta$ -W phase becomes unstable, and subsequently transforms into the more stable  $\alpha$ -W phase.<sup>8</sup> In this letter, we show that under the oblique-angle sputter deposition (OASD), isolated  $\beta$ -W(100) nanorods are formed and are stable against transformation into the  $\alpha$ -W phase.

In our experiment, a dc magnetron sputtering system was used to deposit tungsten films. The films were deposited on oxidized *p*-Si(100) (resistivity 12–25  $\Omega$  cm) substrates ( $\sim 2 \times 2$  cm<sup>2</sup> size) using a 99.95% pure W cathode (diameter  $\sim 7.6$  cm). The substrates were RCA cleaned<sup>12</sup> and mounted on the sample holder located at a distance of 15 cm from the cathode. In the OASD,<sup>13,14</sup> the substrate is tilted so that the angle between the surface normal of the target and the surface normal of the substrate can be large. In our present case, the angle was 87°. The substrate rotation speed was set to 0.5 Hz (30 rpm). In the normal incidence sputter deposition (NISD) the tilt angle was set to 0°, with no sample rotation. The base pressure of  $\sim 2 \times 10^{-6}$  Torr was achieved by a turbomolecular pump backed by a mechanical pump. In all the

deposition experiments, the power was 200 W at an ultra pure Ar pressure of 1.5 mTorr. The deposition rates were measured to be  $\sim 8.5$  nm/min for NISD and  $\sim 5.0$  nm/min for OASD. The thickness of the films ranged from  $\sim 15$  nm up to  $\sim 340$  nm and was determined by a step-profilometer and also verified by scanning electron microscope (SEM) cross-sectional images. The maximum temperature of the substrate during the deposition was measured to be  $\sim 85$  °C. The texture information was studied by a series of x-ray diffraction (XRD) measurements using a Scintag diffractometer with a Cu target operated at 50 kV and 30 mA. The diffractometer was calibrated with respect to the peak positions of a Si calibration standard.

Figures 1(a) and 1(b) show a sequence of x-ray  $\theta$ - $2\theta$  plots of the NISD and OASD tungsten films at different deposition times (thicknesses), respectively. It is realized that  $\alpha$ - and  $\beta$ -phases are present at the initial stages of growth for both normal incidence and oblique-angle depositions. As the growth progresses to larger thickness, the  $\alpha$ -phase for the normal incidence deposition grows faster and the  $\beta$ -phase is suppressed. This behavior is consistent with that reported in the literature.<sup>8,15</sup> On the other hand, we see an opposite behavior for the OASD. The  $\beta$ -phase grows faster as a function of time and the  $\alpha$ -phase almost disappears.

Figure 2 shows SEM top and cross-sectional views of the final films sputter deposited by NI and OA. For the NISD film, the top view (a) shows a featureless structure and the cross section (b) shows the commonly observed columnar structure that is a characteristic of a sputter deposited film. The columnar structure is a result of the shadowing effect due to the fact that not all incident flux arrives perpendicular to the surface. In fact, atoms obey a cosine distribution.<sup>16</sup> The shadowing effect leads to the columnar structure. The columns are not isolated and the film is continuous. On the other hand, the top and cross-sectional views of the OASD film, (c) and (d), respectively, show the structure of the isolated rods. In addition, the top view of a high-resolution SEM image of the isolated nanorods shows fourfold symmetric (110) facets, as illustrated in Fig. 3. Each rod consists

<sup>a)</sup>Electronic mail: karabt@rpi.edu

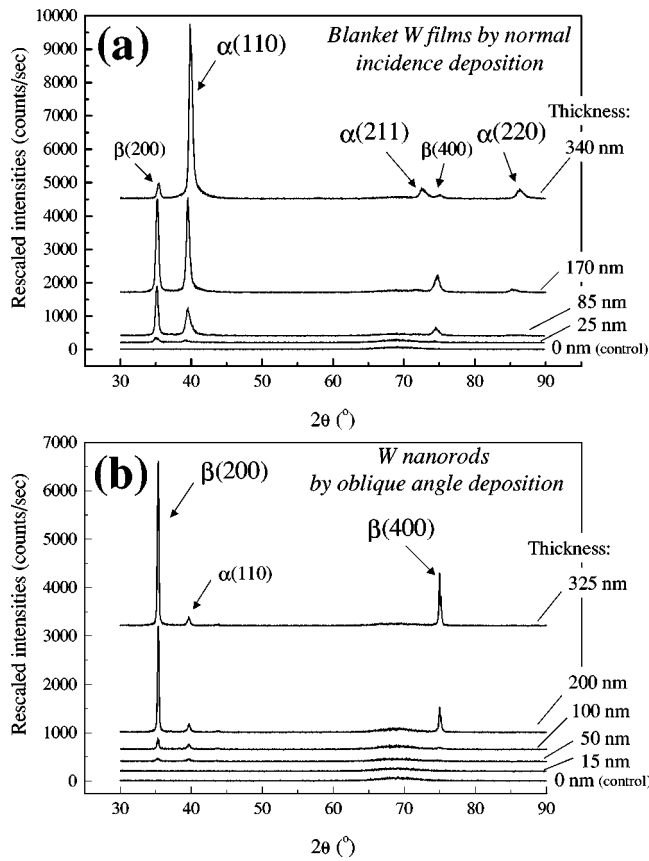


FIG. 1. XRD data of (a) tungsten films sputter deposited at normal incidence, and (b) columnar tungsten films sputter deposited by OASD with substrate rotation for various thicknesses. The y-axis intensity for each spectrum is offset for clarity.

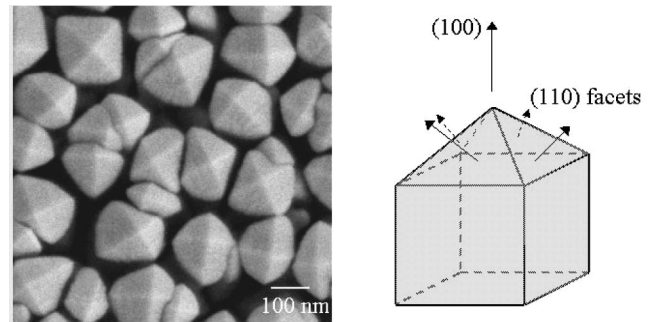


FIG. 3. Top view of high-resolution SEM image of the tungsten nanorods made by OASD showing the fourfold symmetric (110) facets. The top of each rod consists of only one pyramid-shaped faceted structure, suggesting that the nanorods are single-crystal.

of a pyramidal shape facet consistent with the facet of a single-crystal structure.

The mechanism for the  $\alpha$ - and  $\beta$ -W formation has been studied by many authors.<sup>7-9</sup> It is shown that  $\alpha$ -W is the thermodynamically favorable state and the surface adatom mobility is higher than that of the  $\beta$  phase surface.<sup>17</sup> The  $\beta$ -W is considered to be metastable with a poor adatom mobility. Baumann *et al.* performed Monte Carlo simulations and predicted the texture formation.<sup>18</sup> Under the conditions of low substrate temperature and therefore low adatom mobilities, they observed a net flux of surface diffusion from islands of higher adatom surface mobility towards the islands of lower adatom surface mobility and consequent trapping of these adatoms. They also predicted that the obliquely incident atoms would have a higher chance of being captured by islands of lower surface mobility since they can grow taller and can shadow the nearby surface features with higher surface mobility. These predictions may help us understand the

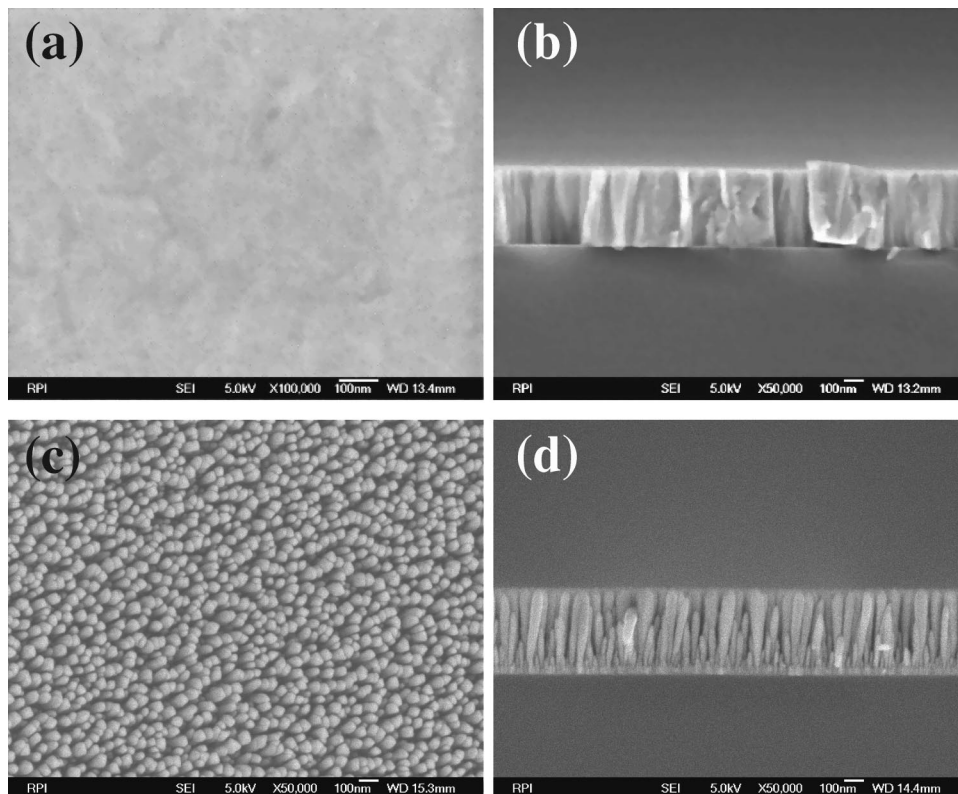


FIG. 2. SEM images of tungsten films made by NISD and nanorods of tungsten made by OASD with substrate rotation: (a) top view and (b) cross-sectional view of a W film, and (c) top view and (d) cross-sectional views of W nanorods.

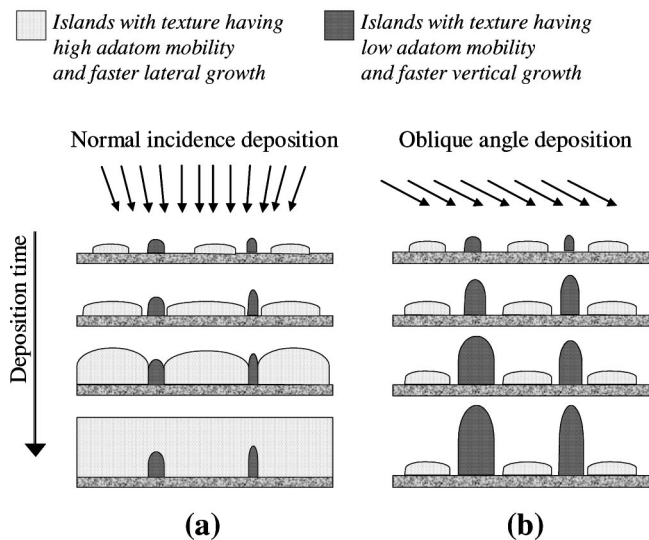


FIG. 4. The cartoon that illustrates the possible texture evolution mechanisms for (a) NISD and (b) OASD.

present experimental observations illustrated in Figs. 4(a) and 4(b).

For the NISD (with a cosine angular distribution of flux), the islands of  $\alpha$ -W grow faster in the lateral directions in the substrate plane and eventually cover up the  $\beta$ -W islands, which is consistent with the predictions of Baumann *et al.* and is shown in Fig. 4(a). On the other hand, during the OASD, due to the extreme shadowing effect we expect that the islands that grow taller in the vertical direction will shadow a considerable amount of surface area in the film. Therefore, as illustrated in Fig. 4(b), we expect a faster growth of the lower mobility  $\beta$ -W islands. The  $\alpha$ -W features are shadowed by the  $\beta$ -W rods and the growth of the  $\alpha$ -W is therefore suppressed. The initial  $\beta$ -W islands are presumably single-crystal islands. These islands serve as seeds to induce the subsequent growth of single-crystal rods.

The fact that the OASD  $\beta$ -W rods stay stable without transforming into the  $\alpha$ -W is quite interesting. It is known in the literature that oxygen plays a role in the stability of  $\beta$ -phase W.<sup>7-9</sup> One possible mechanism for the stable  $\beta$ -phase W(100) formation is that during the OASD, the larger geometrical surface area of nanostructures resulted in the incorporation of excess oxygen in the nanorods to stabi-

lize the otherwise unstable  $\beta$ -phase W(100). Further testing is required to verify this assumption.

In conclusion, we were able to obtain single-crystal  $\beta$ -W(100) nanorods by the oblique-angle sputter deposition technique. We explain our formation of single-crystal  $\beta$ -W(100) nanorods by a combination of a shadowing effect and the difference in the adatom surface mobilities between different crystal planes. We expect these single-crystal  $\beta$ -W(100) rods to possess different field-emission characteristics that may be useful for display applications.

The authors thank Dr. E. Barnat and Y.-G. Zhao for their help with the sputter deposition tool. This work was supported in part by NSF. One of the authors (T.K.) was supported by the Harry F. Meiners Fellowship.

- <sup>1</sup>C.-H. Choi, Y.-T. Jang, B.-K. Ju, Y.-H. Lee, M.-H. Oh, J.-H. Ahn, and N.-K. Min, *SID Digest* **3301**, 369 (2002).
- <sup>2</sup>J. G. Fleming, S. Y. Lin, I. El-Kady, R. Biswas, and K. M. Ho, *Nature (London)* **417**, 52 (2002).
- <sup>3</sup>K. Y. Ahn, *Thin Solid Films* **153**, 469 (1987).
- <sup>4</sup>S. M. Rossmagel, I. C. Noyan, and C. Cabral Jr., *J. Vac. Sci. Technol.* **20**, 2047 (2002).
- <sup>5</sup>M. Itoh, M. Hori, and S. Nadahara, *J. Vac. Sci. Technol. B* **9**, 149 (1991).
- <sup>6</sup>M. S. Aouadi, R. R. Parsons, P. C. Wong, and K. A. R. Mitchell, *J. Vac. Sci. Technol. A* **10**, 273 (1992).
- <sup>7</sup>Y. G. Shen and Y. M. Mai, *Mater. Sci. Eng., A* **28**, 176 (2000).
- <sup>8</sup>I. A. Weerasekera, S. I. Shah, D. V. Baxter, and K. M. Unruh, *Appl. Phys. Lett.* **64**, 3231 (1994).
- <sup>9</sup>M. J. O'Keefe and J. T. Grant, *J. Appl. Phys.* **79**, 9134 (1996).
- <sup>10</sup>R. S. Wagner, A. K. Sinha, T. T. Sheng, H. J. Levinstein, and F. B. Alexander, *J. Vac. Sci. Technol.* **11**, 582 (1974).
- <sup>11</sup>M. Haghiri-Gosnet, F. R. Ladan, C. Mayeux, and H. Launois, *J. Vac. Sci. Technol. A* **7**, 2663 (1989).
- <sup>12</sup>S. A. Campbell, *The Science and Engineering of Microelectronic Fabrication* (Oxford University Press, New York, 1996), p. 341.
- <sup>13</sup>Y.-P. Zhao, D.-X. Ye, G.-C. Wang, and T.-M. Lu, *Nano Lett.* **2**, 351 (2002).
- <sup>14</sup>For a review, see M. Malac, R. Egerton, and M. Brett, *Vacuum Technology & Coating* **2**, 48 (2001).
- <sup>15</sup>I. C. Noyan, T. M. Shaw, and C. C. Goldsmith, *J. Appl. Phys.* **82**, 4300 (1997).
- <sup>16</sup>D. L. Smith, *Thin-Film Deposition: Principles and Practice* (McGraw-Hill, New York, 1995), pp. 96 and 432.
- <sup>17</sup>Y. G. Shen, Y. W. Mai, Q. C. Zhang, D. R. McKenzie, W. D. McFall, and W. E. McBride, *J. Appl. Phys.* **87**, 177 (2000).
- <sup>18</sup>F. H. Baumann, D. L. Chopp, T. Diaz de la Rubia, G. H. Gilmer, J. E. Greene, H. Huang, S. Kodambaka, P. O'Sullivan, and I. Petrov, *MRS Bull.* **26**, 182 (2001).